Theory for displacive excitation of coherent phonons

H.J. Zeiger and J. Vidal
Department of Physics, Massachusetts Institute of Technology, Cambridge, Massachusetts 02139

T.K. Cheng and E.P. Ippen
Department of Electrical Engineering and Computer Science, Massachusetts Institute of Technology, Cambridge, Massachusetts 02139

G. Dresselhaus
Francis Bitter National Magnet Laboratory, Massachusetts Institute of Technology, Cambridge, Massachusetts 02139

M.S. Dresselhaus
Department of Electrical Engineering and Computer Science and Department of Physics, Massachusetts Institute of Technology, Cambridge, Massachusetts 02139
(Received 1 July 1991)

We report femtosecond time-resolved pump-probe reflection experiments in semimetals and semiconductors that show large-amplitude oscillations with periods characteristic of lattice vibrations. Only A_1 modes are detected, although modes with other symmetries are observed with comparable intensity in Raman scattering. We present a theory of the excitation process in this class of materials, which we refer to as displacive excitation of coherent phonons (DECP). In DECP, after excitation by a pump pulse, the electronically excited system rapidly comes to quasiequilibrium in a time short compared to nuclear response times. In materials with A_1 vibrational modes, the quasiequilibrium nuclear A_1 coordinates are displaced with no change in lattice symmetry, giving rise to a coherent vibration of A_1 symmetry about the displaced quasiequilibrium coordinates. One important prediction of the DECP mechanism is the excitation of only modes with A_1 symmetry. Furthermore, the oscillations in the reflectivity R are excited with a $\cos(\omega_0 t)$ dependence, where $t = 0$ is the time of arrival of the pump pulse peak, and ω_0 is the vibrational frequency of the A_1 mode. These predictions agree well with our observations in Bi, Sb, Te, and Ti_2O_3. The fit of the experimental $\Delta R(t)/R(0)$ data to the theory is excellent.

I. INTRODUCTION

Since the early 1980's, many groups have been studying the response of material systems to optical pulses on a femtosecond time scale using optical pulse pump-probe techniques.[1–5] In a number of these experiments, oscillations due to a Raman excitation process are observed in the transmission of probe pulses as a function of time following the exciting pump pulse.[3–5]

Recently, femtosecond pump-probe techniques have been applied to the study of metals and superconductors.[6–10] In pump-probe experiments on a number of conducting or semiconducting materials, oscillations have been observed in reflectivity (or transmission through thin samples) with frequencies that correspond to optical phonon modes of the samples.[11–18] A number of mechanisms have been proposed to explain these oscillations, including impulsive stimulated Raman scattering (ISRS), a nonlinear optical susceptibility mechanism, and the screening of space-charge fields at the surface of semiconducting samples.[12] While these mechanisms appear relevant to the observations in many cases, they are unable to explain the striking results observed in a certain class of materials. These materials are characterized by the observation of Raman-active modes only of A_1 symmetry in pump-probe experiments, even though modes of comparable strength and different symmetries occur in spontaneous and resonant Raman scattering. The materials in which we have made such observations include Sb, Bi,[11,16] Te, and Ti_2O_3.[16,17] Other materials in which only A_1 modes have been reported in pump-probe experiments include semiconducting $YBa_2Cu_3O_{7-\delta}$,[13,15] ϵ-InSe, ϵ-GaSe, and GaS.[15,18]

In this paper we propose a mechanism for the excitation of oscillations in reflectivity or transmission in the class of materials showing only the excitation of A_1 modes. For reasons we will explain shortly, we refer to this phonon generation mechanism as displacive excitation of coherent phonons (DECP). In DECP, only modes of A_1 symmetry are observed. Furthermore, the oscillation amplitudes in the reflectivity R are very large ($\Delta R/R \sim 10^{-2}$–10^{-3}) as compared to the nonoscillatory changes in reflectivity typically observed in metals such as Cu or Au ($\sim 10^{-4}$–10^{-5}). DECP requires a significant absorption at the pump frequency in order to disturb the electronic energy distribution in the material;

 ©1992 The American Physical Society

ISRS does not require absorption in the material.[3,5] The amplitude of oscillations in ΔR observed in DECP for the experiments we report here is linearly proportional to the pump pulse integrated energy for a given beam diameter (see Sec. II). Finally, as we shall see shortly, the oscillations observed in DECP should vary as $\cos(\omega_0 t)$, where ω_0 is the A_1 mode angular frequency, and the time t is measured from the peak of the pump pulse; in ISRS and other nonlinear, impulsive excitation mechanisms, nonresonant excitation leads to oscillations which vary as $\sin(\omega_0 t)$. Resonant ISRS can lead to a $\cos(\omega_0 t)$ dependence of vibrations,[19,20] but then all Raman-active modes should be excited.

A_1 modes are "breathing modes" which do not lower the symmetry of the lattice. Not all lattice structures have A_1 modes of vibration. One way of thinking of a structure with A_1 modes is that it is derived from a "virtual" structure of higher symmetry by nuclear displacements which increase the size of the unit cell. These displacements, which preserve the symmetry of the actual structure, are A_1 symmetry displacements, which have a continuum of possible values. The actual equilibrium value of the A_1 displacements is determined by minimization of the free energy of the system. It therefore follows that the equilibrium positions of nuclei within the unit cell in such structures should be a function of temperature, but should change by displacements of A_1 symmetry. It is also reasonable to expect that if the electronic distribution in such a material is disturbed by a high intensity, short pulse of optical radiation, the equilibrium nuclear coordinates within a unit cell will change by a displacement of A_1 symmetry. The electronically excited system will quickly come to quasiequilibrium on a time scale short compared to the equilibration time for the nuclear system. It might be expected that a $\mathbf{k} \sim \mathbf{0}$ A_1 vibrational mode would then be coherently excited. It is this mechanism which we propose as the source of DECP.

On the other hand, a change in quasiequilibrium nuclear coordinates of any symmetry other than A_1 in an optical pump-probe experiment is highly unlikely. Such a change with electronic excitation could only occur if the material were close to a structural phase transition of that symmetry in its ground state. Therefore the observation of DECP for modes of symmetry other than A_1 could only arise in highly unusual circumstances.

It should be noted that the mechanism we have described for DECP in metals and other conductors with A_1 Raman-active modes is analogous to that proposed for the explanation of oscillations observed in experiments with certain organic molecules.[19,20] In femtosecond optical pump-probe experiments in malachite green, oscillations in transmission were observed when the pump frequency corresponded to an electronic excitation of the molecular system. The explanation proposed[19,20] was that in the electronic excitation process, transitions were produced according to the Franck-Condon principle, leaving the molecules in an excited electronic state and in an excited vibrational state as well because of a displaced equilibrium A_1 coordinate. The coherent phonons excited by the short pump pulse were then detected by the molecular absorption modulation of the organic liquid. There is one important difference, however, between the molecular excitation mechanism and DECP. In the molecular system, the maximum amplitude of vibration is determined by the Franck-Condon principle, so that increasing the pump power increases the number of vibrating molecules, but not the vibrational amplitude. In DECP, the vibrational amplitude increases linearly with pump power.

The existence of an A_1 mode in the material is thus a necessary condition for DECP, but the observation of DECP above noise depends on having a strong dependence of the equilibrium nuclear coordinates on electronic excitation. We will demonstrate that a simple semiclassical model of DECP leads to results consistent with our experimental observations.

II. THEORY

In the model that we consider, an exciting optical pulse of angular frequency ω is incident at time $t = 0$ on the surface of a material with an A_1 mode. The excitation produces a change in reflectivity $\Delta R(t)$ which eventually relaxes back to zero. Earlier pump-probe experiments on conducting materials produced a $\Delta R(t)$ which showed no oscillations, and were interpreted as due to changes in electron temperature ΔT_e produced by the pump pulse.[6,7,9] This interpretation led to measurements of electron-phonon coupling strength λ which were consistent with determinations by other types of experiments.[9]

In the observation of DECP we postulate that the origin of the oscillations in $\Delta R(t)$ is a change in the quasiequilibrium A_1 nuclear coordinate Q_0(t) (where Q_0=0 defines the state before the pulse arrives at the surface). The pulse will change the electron temperature at the Fermi level $\Delta T_e(t)$, but may also produce interband transitions which leave $n(t)$ electrons per unit volume in excited bands. It should be noted that all the materials in which we have thus far observed DECP (Bi, Sb, Te, Ti_2O_3, and preliminary observations in GeTe) are either semimetals or semiconductors, with energy bands above the Fermi level that are accessible to the ~2-eV-pump pulse excitation energy used in these experiments. At the present stage of our study we cannot distinguish whether $n(t)$ or $\Delta T_e(t)$ is the dominant source of the observed DECP. However, the assumption that the change in the quasiequilibrium A_1 nuclear coordinate $Q_0(t)$ is proportional to either $n(t)$ or $\Delta T_e(t)$ leads to a very similar result for $\Delta R(t)$ due to DECP. The derivation that follows is based on $n(t)$ as the source of DECP.

The equation describing the rate of change of $n(t)$ at the surface of the sample is

$$\dot{n}(t) = \rho P(t) - \beta n(t). \tag{1}$$

The first term on the right-hand side of Eq. (1) is the rate of generation of carriers in excited bands, which is assumed to be proportional to the power density, $P(t)$, the energy in the exciting pulse arriving per unit area per unit time at the surface and ρ is a constant of proportion-

ality to be discussed later. The second term in Eq. (1) is the rate of transfer of electrons back to the ground state.

The source of excitation of the A_1 mode is the dependence of the equilibrium A_1 coordinate $Q_0(t)$ on $n(t)$. We take this dependence to be linear:

$$Q_0(t) = \kappa n(t). \tag{2}$$

The equation governing the time dependence of the A_1 coordinate $Q(t)$ is taken as

$$\ddot{Q}(t) = -\omega_0^2[Q(t) - Q_0(t)] - 2\gamma\dot{Q}(t). \tag{3}$$

Here, ω_0 is the angular frequency of the A_1 mode and γ represents a damping constant for the mode. We assume that the change in ω_0 with excitation is small, and can be neglected in first approximation. The general results can be written in the form

$$n(t) = \rho\mathcal{E}_{\text{pump}} \int_0^\infty g(t-\tau)e^{-\beta\tau}\, d\tau \tag{4}$$

and

$$Q(t) = \frac{\omega_0^2\kappa\rho\mathcal{E}_{\text{pump}}}{(\omega_0^2 + \beta^2 - 2\gamma\beta)} \int_0^\infty g(t-\tau)\left[e^{-\beta\tau} - e^{-\gamma\tau}\left(\cos(\Omega\tau) - \frac{\beta'}{\Omega}\sin(\Omega\tau)\right)\right] d\tau. \tag{5}$$

In Eqs. (4) and (5), $P(t)$ has been written as

$$P(t) = \mathcal{E}_{\text{pump}} g(t), \tag{6}$$

where $\mathcal{E}_{\text{pump}}$ is the energy per unit area in the pump pulse and $g(t)$ is a normalized pulse shape function such that

$$\int_{-\infty}^{\infty} g(t)dt = 1. \tag{7}$$

The frequency Ω is given by

$$\Omega \equiv \sqrt{\omega_0^2 - \gamma^2} \tag{8}$$

and

$$\beta' = \beta - \gamma. \tag{9}$$

If R is the unperturbed reflectivity before the arrival of the pump pulse, then the fractional change in reflectivity due to the pump pulse can be written as

$$\frac{\Delta R(t)}{R} = \frac{1}{R}\left[\left(\frac{\partial R}{\partial n}\right) n(t) + \left(\frac{\partial R}{\partial T_e}\right)\Delta T_e(t) + \left(\frac{\partial R}{\partial Q}\right) Q(t)\right]. \tag{10}$$

In Eq. (10) the first term on the right-hand side is due to $n(t)$, the excited band carrier density, defined by Eq. (4); the second term is due to a change in electron temperature; and the third term is due to the change in the A_1 nuclear coordinates, Eq. (5). Our derivation of Eq. (5) is based on the assumption that $n(t)$ is the dominant source driving $Q(t)$, but a very similar formal result is obtained if $Q(t)$ is driven by the temperature change $\Delta T_e(t)$.

Because of the finite width of the probe pulse, what is observed in a pump-probe experiment is not precisely the fractional change in reflectivity given by Eq. (10), but rather an average over the pulse of the form

$$\frac{\overline{\Delta R(t)}}{R} = \frac{1}{R}\left[\left(\frac{\partial R}{\partial n}\right)\overline{n(t)} + \left(\frac{\partial R}{\partial T_e}\right)\overline{\Delta T_e(t)} + \left(\frac{\partial R}{\partial Q}\right)\overline{Q(t)}\right]. \tag{11}$$

The averages in Eq. (11) are given by integrals of the form

$$\overline{H(t)} \equiv \int_{-\infty}^{\infty} H(t')g(t'-t)\, dt', \tag{12}$$

since the pump and probe pulse have the same shape. Here we assume that the perturbation of the system due to a weak probe can be neglected. The expression for $\Delta T_e(t)$ would be formally similar to Eq. (4) for $n(t)$, so that all three of the functions averaged in Eq. (11) are of the form

$$H(t) = \int_0^\infty g(t-\tau)F(\tau)\, d\tau. \tag{13}$$

Thus $\overline{H(t)}$ can be written

$$\overline{H(t)} = \int_{-\infty}^{\infty}\left(\int_0^\infty g(t'-\tau)F(\tau)\, d\tau\right)g(t'-t)\, dt'. \tag{14}$$

Reversing the order of integration, and introducing the variable of integration $x = t' - t$, Eq. (14) can be written as

$$\overline{H(t)} = \int_0^\infty G(t-\tau)F(\tau)\, d\tau, \tag{15}$$

where the pulse autocorrelation function $G(t)$ is defined as

$$G(t) = \int_{-\infty}^{\infty} g(t-\tau)g(\tau)d\tau. \tag{16}$$

Thus, if we continue with the assumption that $n(t)$ is dominant in Eq. (11) and also is the source driving $Q(t)$, then we may write for $\overline{n(t)}$ and $\overline{Q(t)}$ from Eqs. (4) and (5):

$$\overline{n(t)} = \rho\mathcal{E}_{\text{pump}} \int_0^\infty G(t-\tau)e^{-\beta\tau}\, d\tau \tag{17}$$

and

$$\overline{Q(t)} = \frac{\omega_0^2 \kappa \rho \mathcal{E}_{\text{pump}}}{(\omega_0^2 + \beta^2 - 2\gamma\beta)} \int_0^\infty G(t-\tau) \left[e^{-\beta\tau} - e^{-\gamma\tau} \left(\cos(\Omega\tau) - \frac{\beta'}{\Omega} \sin(\Omega\tau) \right) \right] d\tau. \tag{18}$$

The derivatives of R in Eq. (11) appear because R is a function of the complex dielectric constant, which is in turn modulated by n, T_e, and Q. The well-known expression for normal incidence reflectivity R in terms of the dielectric function at pump and probe frequency ω is

$$R = \frac{(n_1 - 1)^2 + n_2^2}{(n_1 + 1)^2 + n_2^2}, \tag{19}$$

where

$$\epsilon(\omega) = \epsilon_1(\omega) + i\epsilon_2(\omega) = (n_1 + in_2)^2. \tag{20}$$

Using Eqs. (11), (17), and (18) we can write

$$\frac{\overline{\Delta R(t)}}{R} = A \int_0^\infty G(t-\tau) e^{-\beta\tau} \, d\tau + B \frac{\omega_0^2}{\omega_0^2 + \beta^2 - 2\gamma\beta} \int_0^\infty G(t-\tau) \left[e^{-\beta\tau} - e^{-\gamma\tau} \left(\cos(\Omega\tau) - \frac{\beta'}{\Omega} \sin(\Omega\tau) \right) \right] d\tau, \tag{21}$$

where

$$A = \frac{1}{R} \left[\left(\frac{\partial R}{\partial \epsilon_1} \right) \left(\frac{\partial \epsilon_1}{\partial n} \right) + \left(\frac{\partial R}{\partial \epsilon_2} \right) \left(\frac{\partial \epsilon_2}{\partial n} \right) \right] \rho \mathcal{E}_{\text{pump}} \tag{22}$$

and

$$B = \frac{1}{R} \left[\left(\frac{\partial R}{\partial \epsilon_1} \right) \left(\frac{\partial \epsilon_1}{\partial Q} \right) + \left(\frac{\partial R}{\partial \epsilon_2} \right) \left(\frac{\partial \epsilon_2}{\partial Q} \right) \right] \kappa \rho \mathcal{E}_{\text{pump}}. \tag{23}$$

For $\beta, \gamma \ll \omega_0$, from the definitions of β' and Ω, the surviving oscillatory term in Eq. (21) is $\cos(\omega_0 \tau)$. For sufficiently narrow pump and probe pulses, $G(t)$ can be taken as a δ function, and Eq. (21) becomes

$$\frac{\overline{\Delta R(t)}}{R} = A e^{-\beta t} + B \frac{\omega_0^2}{\omega_0^2 + \beta^2 - 2\gamma\beta} \left[e^{-\beta t} - e^{-\gamma t} \left(\cos(\Omega t) - \frac{\beta'}{\Omega} \sin(\Omega t) \right) \right], \tag{24}$$

where Ω is given by Eq. (8) and β' is given by Eq. (9).

From Eq. (24) we note that for a large decay constant β, the oscillatory term is depressed due to the factor

$$\frac{\omega_0^2}{\omega_0^2 + \beta^2 - 2\gamma\beta}.$$

This is to be expected since a large β means a rapid return of the quasiequilibrium displacement to zero, suppressing the oscillations. Furthermore, a large value of β can contribute a $\sin \Omega t$ term if β'/Ω is not negligibly small, yielding an oscillation with a phase shifted from a simple $\cos \Omega t$. Finally, if the width of the autocorrelation function is not narrow compared to the period of oscillation $1/\omega_0$, then we must revert to Eq. (21), and the oscillatory terms will be suppressed, as expected physically.

Since $(\partial\epsilon/\partial Q)$ is related to the strength of the Raman scattering at the frequency of the probe pulse, from Eq. (23), a condition for the *detection* of strong A_1 oscillations in ΔR is the presence of a strong Raman scattering cross section at frequency ω. However, the *excitation* of A_1 oscillations by the mechanism we have discussed is not directly related to the Raman process itself. The fact that both A and B are proportional to $\mathcal{E}_{\text{pump}}$ indicates that the strength of the DECP signal as well as the back-

TABLE I. Values of fitting parameters for the DECP model and literature Raman data.

Material	Pump-probe data							Raman data	
	A	B	C	τ_{el}[a] (ps)	τ_{ph}[a] (ps)	$\omega_0/2\pi$ (THz)	Φ (degrees)	$\omega_0/2\pi$ (THz)	τ_{ph} (ps)
Sb	$+2.5 \times 10^{-3}$	$+2.7 \times 10^{-2}$	-2.2×10^{-5}	1.67	2.90	4.5 ± 0.1	$+3 \pm 4$	4.50[b]	2.1
Bi	-4.6×10^{-3}	$+3.1 \times 10^{-3}$	-1.3×10^{-3}	10.3	2.41	2.9 ± 0.1	-13 ± 13	2.94[b]	1.5
Te	-6.6×10^{-3}	$+1.4 \times 10^{-2}$	$+3.2 \times 10^{-4}$	0.63	1.26	3.6 ± 0.1	$+7 \pm 9$	3.61[c]	1.5
Ti_2O_3	$+2.6 \times 10^{-2}$	-5.7×10^{-2}	-3.7×10^{-3}	0.40	1.59	7.0 ± 0.1	-20 ± 10	7.14[d]	0.2

[a] Values for relaxation time are accurate within 10%. Values of τ_{ph} are given for room temperature.

[b] Reference 21.

[c] Reference 22.

[d] Reference 23.

ground signal is proportional to the integrated energy in the pump pulse for a fixed beam diameter.

The parameters A and B are themselves of considerable interest. As shown in Table I, which will be discussed further in Sec. IV, there seems to be no correlation between the signs of A and B for the four materials we have studied in detail thus far. In earlier experiments on metals and superconductors,[9] the sign of A was shown to depend on the frequency ω, due to the dependence of $\partial\epsilon_1/\partial\Delta T_e$ and $\partial\epsilon_2/\partial\Delta T_e$ on the pulse frequency. From Eq. (23), the sign and magnitude of B depend on $\partial\epsilon_1/\partial Q$ and $\partial\epsilon_2/\partial Q$. Spontaneous Raman scattering gives no information on the signs of these quantities, since the Raman cross section is proportional to $|\partial\epsilon/\partial Q|^2$. A study of the frequency dependence of B, should thus yield further insight into the mechanism of DECP.

It should be noted that the formal result in Eq. (21) would be essentially the same if only $\Delta T_e(t)$ produced both a direct term proportional to $\Delta T_e(t)$ and an indirect term proportional to $Q(t)$. In that case, $\partial\epsilon_1/\partial n$ and $\partial\epsilon_2/\partial n$ in Eq. (22) would be replaced by $\partial\epsilon_1/\partial\Delta T_e$ and $\partial\epsilon_2/\partial\Delta T_e$, respectively. Also, κ in Eq. (23) would be defined by a new relation

$$Q_0(t) = \kappa\,\Delta T_e(t), \tag{25}$$

replacing Eq. (2). The parameter β in Eq. (21) would then be proportional to the electron-phonon coupling constant λ. At any rate, as we discuss below, only a single exponential decay constant β is needed to obtain a good fit of Eq. (21) to experiment (although as discussed in Sec. IV, in some cases different long and short time values of γ are observed experimentally).

A knowledge of ϵ_1 and ϵ_2 at the frequency ω allows a determination of R, $\partial R/\partial\epsilon_1$, and $\partial R/\partial\epsilon_2$. Also ϵ_1 and ϵ_2 are known for many materials from analysis of reflectivity experiments. The remaining undetermined parameters in Eqs. (22) and (23) are $\partial\epsilon_1/\partial n$, $\partial\epsilon_2/\partial n$, $\partial\epsilon_1/\partial Q$, $\partial\epsilon_2/\partial Q$, ρ, and κ. In principle, some information is available on $\partial\epsilon/\partial Q$, since the Raman scattering intensity is proportional to $|\partial\epsilon/\partial Q|^2$. In practice, however, it is difficult to measure absolute Raman cross sections.

If the source of Eq. (21) is indeed the excitation of carriers $n(t)$, then the parameter ρ appearing in Eqs. (22) and (23), and defined in Eq. (1), can be examined in more detail using the following argument. If $P(t)$ is the power density incident on the surface from outside, then the power density inside the material at the surface is

$$P_{\text{inside}}(0,t) = (1-R)P(t). \tag{26}$$

The power density in the electromagnetic field decays as

$$P_{\text{inside}}(z,t) = P_{\text{inside}}(0,t)e^{-2(n_2\omega/c)z}. \tag{27}$$

The rate of power dissipation per unit volume at the surface is then

$$\left|\frac{\partial P_{\text{inside}}}{\partial z}\right|_0 = P_{\text{inside}}(0,t)\times 2n_2\omega/c. \tag{28}$$

Power dissipation is due to electrons absorbing quanta of energy $\hbar\omega$, so that if the main contribution to absorption is via interband transitions, then the rate of interband transitions of electrons per unit volume at the surface is

$$\frac{dn}{dt} = \frac{1}{\hbar\omega}\left|\frac{dP_{\text{inside}}}{dz}\right|_0 = \frac{2n_2}{\hbar c}P_{\text{inside}}(0,t) = \frac{2n_2}{\hbar c}(1-R)P(t). \tag{29}$$

From the definition of ρ in Eq. (1), ρ is given by

$$\rho = f\,\frac{2n_2}{\hbar c}(1-R), \tag{30}$$

where f is the fraction of electrons transferred in the interband transition that are left in excited bands after quasiequilibration of the electrons. As a check on Eq. (28) we note that if $P_{\text{inside}}(0,t)$ is written in terms of the time average of the Poynting vector at the surface, we obtain

$$\left|\frac{dP_{\text{inside}}}{dz}\right|_0 = \frac{\epsilon_2\omega}{2}|E_{\text{inside}}(t)|^2 \tag{31}$$

as expected.

III. THERMODYNAMIC RELATIONS

In the spirit of Landau theory we can relate the parameter κ appearing in Eq. (2) to quantities arising in a thermodynamic description of quasiequilibrium. We suppose that the (lower symmetry) material under study is generated from a "virtual" material of higher symmetry by a displacement of nuclear coordinates q corresponding to an A_1 mode of the real, lower symmetry material. Before the incidence of the pump pulse, the free energy per unit volume of the system as a function of coordinate q can be written as an expansion of the form

$$F = -an_0q^2 + bn_0q^4 + \cdots, \tag{32}$$

a series in even powers of q. Here n_0 is the number of unit cells per unit volume. The equilibrium value of q, obtained by setting $\partial F/\partial q = 0$ is

$$|q_{\text{eq}}(0)| \cong \left(\frac{a}{2b}\right)^{1/2}. \tag{33}$$

This result is only reasonable for materials such as Bi or Sb, where the equilibrium displacement $q_{\text{eq}}(0)$ from the higher symmetry structure is small (see Sec. V).

The free energy can be written for q near $q_{\text{eq}}(0)$ as

$$F = -\frac{a^2}{4b}n_0 + 2an_0[q - q_{\text{eq}}(0)]^2 + \cdots. \tag{34}$$

If the motion of the nuclear system in the A_1 mode is characterized by an effective mass per unit cell μ, then the equation of motion for the A_1 mode for small displacement is

$$\mu n_0\ddot{q} = -\frac{\partial F}{\partial q} = -4an_0[q - q_{\text{eq}}(0)], \tag{35}$$

yielding the characteristic A_1 frequency

$$\omega_0 = \left(\frac{4a}{\mu}\right)^{1/2}. \tag{36}$$

For a material like Bi or Sb, knowledge of $q_{eq}(0)$, μ, and ω_0 then determines a and b.

Next, we assume that the arrival of the pump pulse at the surface produces a number of carriers per unit volume n, and the free energy per unit volume as a function of q can now be written as

$$F(n) = -an_0q^2 + bn_0q^4 + (c_1 + c_2q^2)n + \cdots . \quad (37)$$

In Eq. (37) we have modeled the n-dependent term as consisting of two parts. The first, due to transfer of electrons across a gap to an excited band, is c_1n. The second, due to the modulation of that gap by the displacement q, is c_2q^2n. The parameter c_2 may be positive or negative, depending on the material. For quasiequilibrium, the condition that $\partial F(n)/\partial q = 0$ now yields the relation

$$q_{eq}(n) = \left(\frac{a}{2b} - \frac{c_2}{2b}\frac{n}{n_0}\right)^{1/2} \cong q_{eq}(0) - \frac{c_2}{2a}q_{eq}(0)\frac{n}{n_0}. \quad (38)$$

Thus, from the definition of κ in Eq. (2) we obtain

$$\kappa = \frac{Q_0}{n} = \frac{q_{eq}(n) - q_{eq}(0)}{n} = -\frac{c_2}{2a}\frac{q_{eq}(0)}{n_0}. \quad (39)$$

The only undetermined parameter in Eq. (39) is c_2.

For $q \sim q_{eq}(n)$, the free energy can be written

$$F(n) = -\left(a - \frac{c_2n}{n_0}\right)^2\left(\frac{n_0}{4b}\right) + c, n + 2\left(a - c_2\frac{n}{n_0}\right)n_0[q - q_{eq}(n)]^2 + \cdots . \quad (40)$$

Equation (40) predicts a small change in ω_0 due to the excitation of n electrons per unit volume. Even if the change in ω_0 is so small that it is undetectable within experimental accuracy, yet the excitation of n electrons per unit volume could lead to a large observable DECP because of the sensitivity of the dielectric behavior of the material to the A_1 nuclear displacement.

If ΔT_e rather than n in Eq. (37) is the source of the change in quasiequilibrium q due to the exciting pulse, the formal result for κ in Eq. (39) is the same.

On the assumption that the excitation of carriers to an excited band drives Q_0, it is possible to obtain a rough estimate for $Q_0/q_{eq}(0)$ for Bi and Sb by the following argument. c_2q^2 in Eq. (37) is the extra energy increase due to the displacement q when one electron is transferred to an excited band. A measure of c_2 can be obtained by equating the equilibrium value of c_2q^2 to a characteristic energy splitting Δ produced in the band structure by the symmetry-lowering displacement in the crystal (see discussion in Sec.V). The splitting Δ can be estimated from the splittings produced at the L point or T point assuming the excited carriers arise mainly at these points in the Brillouin zone. We then write

$$c_2q_{eq}^2(0) = \Delta. \quad (41)$$

Substituting for c_2 from Eq. (41) and for a from Eq. (36) we obtain

$$Q_0 \equiv q_{eq}(n) - q_{eq}(0) = -\frac{c_2}{2a}q_{eq}(0)\frac{n}{n_0} = \frac{-2\Delta}{q_{eq}^2(0)\mu\omega_0^2}q_{eq}(0)\frac{n}{n_0}. \quad (42)$$

It is convenient to write the ratio $Q_0/q_{eq}(0)$ in the dimensionless form

$$Q_0/q_{eq}(0) = \frac{-2}{(2\pi)^2}\frac{\Delta}{m_0c^2}\frac{m_0}{\mu}\frac{1}{q_{eq}^2(0)\lambda_0^{-2}}\frac{n}{n_0}, \quad (43)$$

where m_0 is the free electron mass and λ_0^{-1} is the A_1 mode frequency in wave numbers. Substituting known quantities in Eq. (43) we obtain the result

$$Q_0 = -gq_{eq}(0), \quad (44)$$

where

$$g \cong 5.4 \times 10^5\Delta(\text{eV})\frac{1}{\mu(\text{MW})}\frac{1}{q_{eq}^2(0)(\text{Å}^2) \times \lambda_0^{-2}(\text{cm}^{-2})}\frac{n}{n_0} \quad (45)$$

and μ is measured in molecular weight (MW) units per unit cell.

The maximum value of n can be estimated by integrating Eq. (29) for dn/dt over the pump pulse. The result is

$$n_{max} \cong \rho\mathcal{E}_{pump}, \quad (46)$$

where ρ is given by Eq. (30), and $\mathcal{E}_{pump}$ is the energy per square cm in the incoming pump pulse. For a 10-pJ pulse focused to a 2-μm diameter spot size (see Sec. IV), we obtain $\mathcal{E}_{pump} = 3.2 \times 10^3$ ergs/cm^2, so that

$$n_{max} \cong 2.0 \times 10^{20} f\, n_2(1 - R)\ \text{cm}^{-3}. \quad (47)$$

Before applying the result for Q_0 to specific materials, it is useful for comparison to obtain an expression for the mean squared value of the ground-state displacement of the A_1 mode $\overline{q^2}$, given by the relation

$$\tfrac{1}{2} \times 4a\overline{q^2} = \tfrac{1}{2}\hbar\omega_0. \quad (48)$$

Substituting for a from Eq. (36) we obtain

$$\overline{q^2} = \frac{\hbar}{\mu\omega_0} = \frac{1}{2\pi}\frac{\alpha a_0}{\lambda_0^{-1}}\frac{m_0}{\mu}, \quad (49)$$

where $\alpha = e^2/(\hbar c)$ is the fine structure constant and $a_0 = \hbar^2/(me^2)$ is the Bohr radius. Substituting the values of these constants gives the result for $q_0 \equiv (\overline{q^2})^{1/2}$,

$$q_0 \cong 5.67\left(\frac{1}{\mu(\text{MW})\lambda_0^{-1}(\text{cm}^{-1})}\right)^{1/2}\ \text{Å}. \quad (50)$$

The average harmonic oscillator quantum number l for the A_1 mode associated with the maximum displaced quasiequilibrium coordinate Q_{0max} [for $Q_{0max} > q_{eq}(0)$] is given by the relation

$$(l + \tfrac{1}{2})\hbar\omega_0 = \tfrac{1}{2} \times 4aQ_{0max}^2. \quad (51)$$

Combining Eqs. (48) and (51) we have

$$(l+\tfrac{1}{2}) = \frac{1}{2}\frac{Q_{0\max}^2}{q_0^2} = \frac{1}{2}g_{\max}^2\frac{q_{eq}^2(0)}{q_0^2}, \quad (52)$$

where $g_{\max}$ is given by Eq. (45) evaluated for $n = n_{\max}$.

We apply these relations to the case of Bi. For the A_1 mode of Bi, $\lambda_0^{-1} = 96\ \mathrm{cm}^{-1}$, and the effective mass $\mu(\mathrm{MW})/2 = 104.5$. With these values we find from Eq. (50) that $q_0 \cong 0.056$ Å. The values of $q_{eq}(0)$ for Bi (which we define as the decrease in the distance between paired planes from their simple cubic distances) is 0.378 Å.[24] The number of unit cells (containing 2 Bi atoms) per unit volume is $n_0 = 1.4 \times 10^{22}\mathrm{cm}^{-3}$. The relevant splittings, Δ, for Bi are ~ 0.41 eV at the L point, and ~ 0.68 eV at the T point.[25] Taking the smaller of these values for Δ we obtain from Eq. (45)

$$g_{\max} \cong 1.6\frac{n_{\max}}{n_0}. \quad (53)$$

We note that for $n_{\max}/n_0 \sim 1$, $g_{\max} \sim 1$, and $Q_{0\max} \sim -q_{eq}(0)$, roughly what might be expected. The value of $n_{\max}$ can be evaluated from Eq. (47) using $n_2 \cong 5$, $R \cong 0.7$, and we obtain $n_{\max} \cong 3 \times 10^{20} f$. This gives $g_{\max} = 0.034f$. The value of $Q_{0\max}$ from Eq. (44) is then $Q_{0\max} \simeq -0.013f$ Å. This magnitude of displacement is less than q_0 even for $f \sim 1$, so that from Eq. (52), the average value of the oscillator quantum number l is much less than 1.

In spite of the small magnitude of $Q_{0\max}$, the effect produced in DECP is large because the vibrational excitation is coherent, and the dielectric response is sensitive to the coherent vibrational amplitude. A well-known property[26] of the quantum mechanical harmonic oscillator of angular frequency ω_0 is the fact that an initial displaced Gaussian wave packet centered at a point z_0 from the origin has a probability density which is a similar Gaussian centered at time t at a point $z = z_0\cos(\omega_0 t)$. Thus, in DECP the initial displacement $Q_{0\max}$ of the Gaussian wave function for the $l = 0$ state leads to a coherent vibration about the new equilibrium coordinate of the A_1 mode, producing a large modulation of the reflectivity R.

IV. EXPERIMENTAL RESULTS

The samples that were studied in our initial work[11,14] were in a variety of forms, including polycrystalline films (Bi), polycrystalline bulk samples (Bi and Sb), as well as single crystals (Bi, Sb, and Te).

DECP was observed in all of the Bi and Sb samples, although the best signal-to-noise ratios were achieved with single crystals. With regard to sample preparation, the bismuth and antimony single crystals were cleaved along the trigonal face. No cleaving was necessary with the Te single crystal because it had a naturally exposed trigonal face with an optical quality surface. Bismuth films of various thicknesses (800, 1600, 5000 Å) were vacuum deposited in a single pump-down by selective masking onto glass slides, using 99.999% pure bismuth metal as the starting material. The samples of Ti_2O_3 were cut from high quality single crystals of Ti_2O_3 and polished.[27]

The short pulse laser that we used in these experiments is a dispersion-compensated colliding-pulse mode-locked (CPM) laser source.[28] Our CPM laser source generates a train of stable transform-limited pulses at 1.98 eV, measured to be as short as 55 fs in duration, using a standard second harmonic generation method for autocorrelation.[1] The CPM has an average output power of 5 mW and has a repetition rate of 100 MHz.

Our time-resolved impulsive scattering experiment belongs to a class of well-established "pump-probe" type experiments.[1] In a "pump-probe" experiment, each output pulse from the CPM laser is split into two beams, yielding a sample excitation pulse (referred to as the "pump") and a sample measuring pulse (referred to as the "probe"). (See Fig. 1.) The pump and probe travel along two separate beampaths and are focused to the same spot on the sample. By varying the relative length differences between the pump beampath and the probe beampath (with 0.2-μm resolution), an effective delay τ between the arrival time of the pump and the arrival time of the probe can be introduced (0.67-fs resolution). The pump pulse is intense in order to disturb the system from equilibrium, while the probe pulse is weaker to minimize the disturbance that it produces. By sweeping the time delay of the probe, we can systematically scan the entire reflectivity response of the nonequilibrium state as a function of time after arrival of the pump pulse.

The signature of DECP in our experiments is an oscillatory feature in ΔR with a period corresponding to an A_1 Raman-active mode that is found through reflection pump-probe measurements. The data shown in Fig. 2 were obtained with a pump-pulse width of 60 fs with $\sim$ 10-pJ-pulse energy focused onto a $\sim$ 2-μm-diameter spot size. Our pump-probe experiments in Bi, Sb, Te, and Ti_2O_3 all show similar features. In Fig. 2 the reflectivity changes $\Delta R/R$ are plotted as a function of time delay for each material. In each of these pump-probe scans, oscillations characteristic of the material are found superimposed on decaying backgrounds. The fractional changes in the power of the reflected probe pulse ($\Delta R/R$) associated with the coherent generation of optical phonons have been typically on the order of $\sim 10^{-2}$ for antimony, tellurium, and Ti_2O_3, and $\sim 10^{-3}$ for bis-

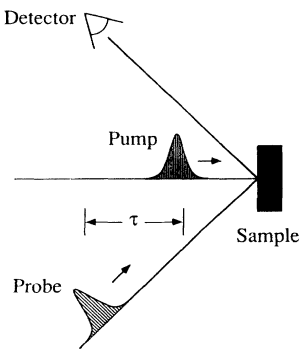

FIG. 1. Schematic diagram of the pump-probe technique used for measurement of the change in reflectivity associated with the coherent generation of optical phonons.

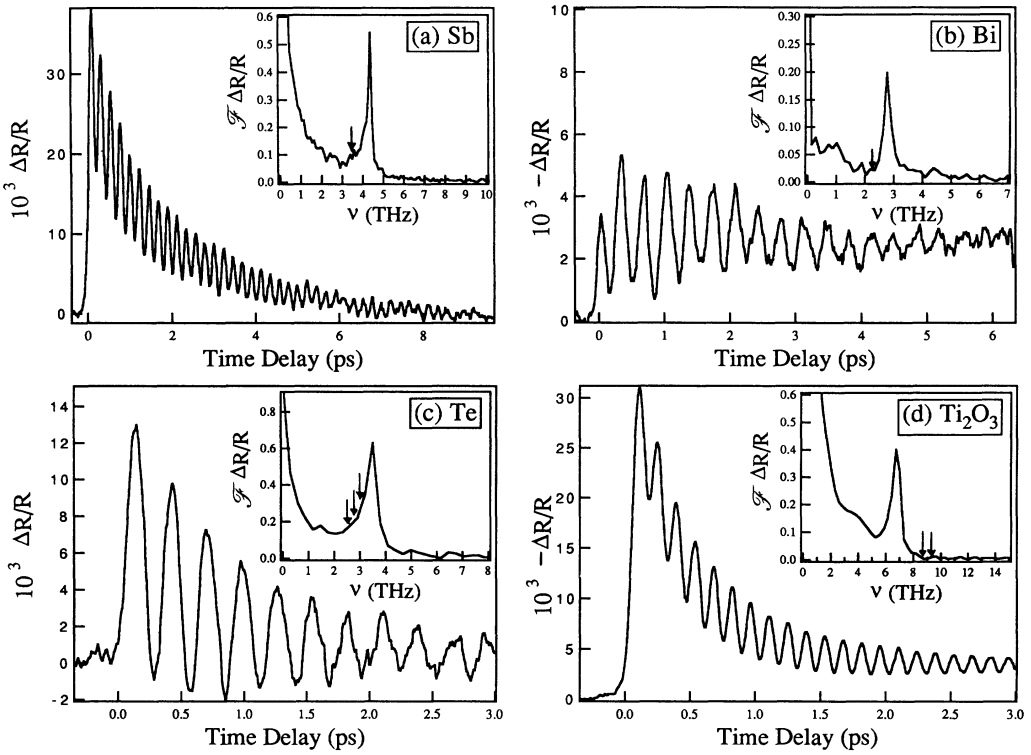

FIG. 2. Observations of the coherent generation of optical phonons in Bi, Sb, Te, and Ti_2O_3 using the pump-probe experiments. In each case a Fourier transform of the data is shown as an inset. Arrows indicate the positions of Raman active lines which appear in spontaneous Raman scattering and have intensities comparable to those of A_1 or A_{1g} modes but do not appear in the Fourier-transform spectrum.

muth. These changes in $(\Delta R/R)$ are large relative to typical femtosecond pump-probe experiments on metals[6] and semiconductors.[12]

Fourier transforms of the oscillatory data shown in Fig. 2 yield a single sharp frequency for each material, and the results are presented in the insets to Fig. 2. In each case the observed frequency is in excellent agreement with the totally symmetric A_1 breathing phonon modes previously determined by Raman spectroscopy[21–23] (see Table I), except for Ti_2O_3 where the agreement is fair. This observation is consistent with DECP, which modifies the index of refraction in the illuminated volume, thereby modifying the optical reflectivity, the observable that we measure. In the case of Ti_2O_3 we attribute the small disagreement to the sensitivity of the Raman frequency to lattice temperature. The spontaneous Raman frequency of this mode is known to drop by as much as 10% as the temperature approaches the range where a "soft" phase transition with no change in lattice symmetry occurs.[23]

In our analysis of the pump-probe data, we have separated the total reflectivity response of the sample into the sum of two contributions, one due to the carriers and the other due to the phonons. The carrier response may be modeled at the simplest level as a step decay exponential $[e^{-\beta t}u(t)]$ convolved with the experimental pulse autocorrelation function $G(t)$. Subtracting this carrier response from the total response yields the phonon response which can be described by a homogeneous classical equation of motion for the phonon vibrational amplitude, Eq. (3) without the driving term. The solution to the equation of motion is a damped sinusoid of an arbitrary phase (Φ). If the phonon excitation mechanism were ISRS then the phonon response would follow a sine dependence, which we write, for purposes of comparison with the theory of Sec. II, in the form $\cos(\omega_0 t + \Phi)$, with $\Phi = \pi/2$. However, if the phonon excitation mechanism were to involve the DECP mechanism, then, as we have seen in Sec. II, the oscillatory signal would show a $\cos(\omega_0 t)$ dependence ($\Phi = 0$ provided $\beta/\omega_0 \ll 1$). In Fig. 3 we determine the phase of the oscillation in Sb by extrapolating the oscillation back to zero time delay. To carry out this extrapolation, the forward trace is taken in the normal manner. The roles of the pump and probe are then reversed, and zero time delay is precisely determined by locating the point of mirror symmetry.[16,29] Because of the weakness of the probe pulse as a pump, the dashed trace in Fig. 3 required upscaling to match the strength of the solid trace. Clearly, because a valley, and not a midpoint, of the oscillation is coincident with zero time delay, we conclude that the phonon response closely follows a cosinusoidal dependence. In a similar way we have analyzed the pump-probe data for all four materials and have concluded that in each case the phonon response follows a cosine dependence, consistent with the DECP mechanism.

Having established that the DECP oscillations do indeed behave as $\cos\omega_0 t$, we obtained the best least squares

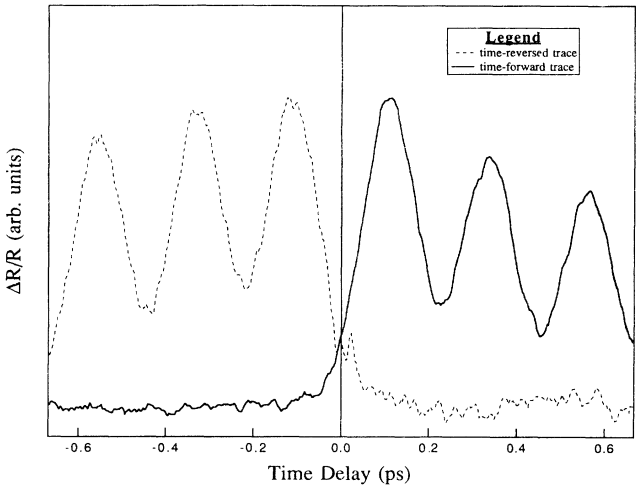

FIG. 3. Two typical pump-probe data traces obtained by chopping the pump beam (solid trace) and the probe beam (dashed trace). Zero time delay is determined by the vertical line of symmetry for the peaks and valleys of the two traces.

fit to our data using Eq. (21) and the experimentally known autocorrelation function $G(t)$. In obtaining our fits, it was necessary to add to Eq. (21) a constant background level which is taken as

$$C\int_0^\infty G(t-\tau)\,d\tau.$$

This is a measure of the long-time residual background signal in our experiments. Such background signals have been observed in our earlier study of metals and superconductors, where they have been attributed to overall lattice heating of the samples.[8–10] In the data shown in Fig. 2, the background might also have a contribution due to a slow return of electrons from excited bands to the ground state. Values of the parameters, A, B, C, $\tau_{\rm el} \equiv 1/\beta$, and $\tau_{\rm ph} \equiv 1/\gamma$ for Bi, Sb, Te, and Ti_2O_3 are all listed in Table I. Figure 4 shows the sensitivity of the fit to the phase angle Φ for the oscillatory part of the data for Sb.

It is interesting to note that for the case of Sb, the fit of the data, with the parameters of Table I, is excellent for the first ~ 5 ps after the pump pulse; but after that time, a clear experimental phonon signal is observed that is decaying more slowly than predicted. A similar effect has been observed by Kurz and co-workers in other materials.[30] The values of $\tau_{\rm ph}$ in Table I which fit the data for short times are somewhat smaller than expected from the spontaneous Raman linewidth.[11] In DECP, the electronic system is initially in a highly excited state. The short time, excess phonon damping implied by the pump-probe data could be due to the interaction of the coherent phonon state with the excited electron gas or phonons emitted in the equilibration process. There could also be an excess damping due to the inclusion in the coherent state wave function of high vibrational quantum-state contributions.

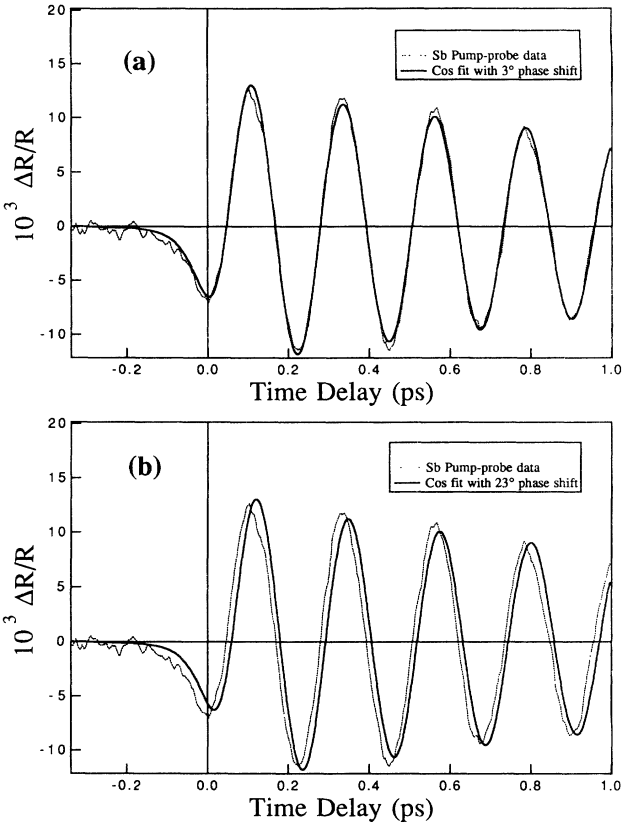

FIG. 4. The oscillatory contribution to the pump-probe data (dashed curve) and the corresponding fit (solid curve) obtained by convolving the measured pulse autocorrelation with an exponentially damped cosine, phase shifted by (a) $\Phi = 3°$ and (b) $\Phi = 23°$ from $\cos\omega_0 t$ behavior.

V. DISCUSSION

A convenient way of identifying potential materials which can yield observable DECP in pump-probe experiments is provided by the handbook compiled by Pearson.[31] In this compendium, materials are classified according to their detailed crystal structure, including the positions of nuclei within a unit cell. Those classes of materials derived by arbitrary displacement of coordinates of certain nuclei can be identified by the presence of parameters x, y, z, in the labeling of their position in the unit cell. But the degree of freedom in the position of nuclei in the unit cell is precisely the condition for the existence of an A_1 mode of displacement. Furthermore, the number of A_1 modes for a structure is the same as the number of parameters x, y, ..., labeling nuclear positions. If a material has several A_1 modes, then each is potentially excitable in a pump-probe experiment to the extent that electronic excitation of the material produces a $Q_0(t)$ for that mode [i.e., each A_1 mode has its own value of κ in Eq. (2)]. Kurz[15] has reported the observation of two A_1 modes in transmission for femtosecond pump-probe experiments in ϵ-InSe. Of course, from Eq. (21), the higher frequency A_1 modes will tend

to be suppressed because they approach the bandwidth limit of the pulse autocorrelation function $G(t)$.

Another requirement for the excitation of an A_1 mode by the present mechanism in an optical pump-probe experiment is that the material studied is at least weakly absorbing at the optical pulse frequency. This is necessary in order that either an electron temperature change $\Delta T_e(t)$ or an interband electron excitation $n(t)$ occurs. Such a requirement does not hold for the Raman excitation process, where optical mode excitation has been observed in organic materials at probe frequencies where the material is transparent.[3,5]

A microscopic mechanism for the observation of DECP in Bi and Sb is suggested by a simple model for the structure of Bi due to Cohen and Blount (CB).[24] The structure can be thought of as derived from a simple cubic by a slight pairing of hexagonal planes along a $\langle 111 \rangle$ cubic axis, plus additional small trigonal distortions which are assumed to play a less essential role. The bismuth atom consists of a core and an outer $6s^2 6p^3$ electronic structure. Because the atomic $6s$ and $6p$ levels are well separated in energy, CB assume that the band structure of bismuth for a simple cubic lattice would consist of a Brillouin zone of p bands which could hold six electrons per atom. These bands would be half full. Born[32] has shown, however, that a simple cubic structure for a monatomic solid is unstable. A small pairing of hexagonal planes along a $\langle 111 \rangle$ axis would lower the energy of the system. This would also double the unit cell size and open a small gap in the bands, lowering additionally the total band energy of the electrons. At the same time, the repulsive core potential would eventually increase the energy, and the pairing displacements would stop when the free energy was a minimum. The pairing displacements are, of course, the A_{1g} displacements of bismuth. In this model, on the arrival of the pump pulse, electrons would be excited into band states higher in energy, which would presumably reduce the free energy advantage of plane pairing, thus reducing the quasiequilibrium displacement of planes and exciting an A_{1g} oscillation. This would imply a positive value of c_2 defined in Eq. (37). This argument neatly parallels the free energy discussion of Sec. III.

The basic concepts of the CB model can also be applied to explain the observation of DECP in an optical pump-probe experiment in Te. The crystal structure of Te can be thought of as derived from a hexagonal close-packed lattice by small distortions which consist, in this case, of shear displacements of hexagonal planes in such a way that Te atoms form spirals with axes along the c axis. This triples the unit cell of Te, producing subbands which can each hold two of the four Te electrons per atom, with energy gaps between. The final value of the shear displacement is determined by the competition between the electronic free energy decrease, and the core energy increase. Finally, excitation of electrons into excited bands decreases the free energy advantage of the shear displacement as discussed in Sec. III, producing a new displaced quasiequilibrium value of the A_1 coordinate, Q_0, and thus exciting the A_1 optical mode.

The case of Ti_2O_3, which has the corundum structure, is of special interest, since this material is known to undergo a "soft" phase transition at ~450 K, over a temperature interval of ~50 K, with no change in crystal symmetry. The transition is accompanied by a drop in resistivity of an order of magnitude, and an increase in Ti-Ti pair distances along the c axis of ~1.5% as the temperature is raised. The transition has been shown[33,34] to involve a crossing of bands and thus a redistribution of electrons. It is therefore not surprising that a large DECP effect has been observed at room temperature in Ti_2O_3, with $\Delta R/R$ changes of $\sim 3 \times 10^{-2}$. The A_{1g} mode observed in DECP corresponds to the lowest frequency A_{1g} mode observed in spontaneous Raman scattering. Interesting effects are seen in pump-probe experiments as the temperature is raised through the transition,[17] and a detailed analysis will be forthcoming.

ACKNOWLEDGMENTS

We are grateful to Dr. Alan Strauss of Lincoln Laboratory for his continuing interest in this work, and for his help in providing us with appropriate samples. Portions of this work were supported by Grant Nos. NSF-87-19217 DMR, NSF88-19896-DMR, AFOSR F49620-88-C-0089, and JSEP Contract Nos. DAAL 03-89-C0001, and DAAL 03-86-002.

[1] E. P. Ippen and C. V. Shank, in *Ultrashort Light Pulses*, edited by S. L. Shapiro (Springer-Verlag, Berlin, 1984), Chap. 3, p. 83.

[2] *Ultrafast Phenomena VII*, edited by C. B. Harris, E. P. Ippen, G. A. Mourou, and A. H. Zewail (Springer-Verlag, Berlin, 1990), Series in Chemical Physics. See also earlier volumes of this series.

[3] S. De Silvestri, J. G. Fujimoto, E. P. Ippen, E. B. Bamble Jr., L. R. Williams, and K. A. Nelson, Chem. Phys. Lett. **116**, 146 (1985).

[4] M. J. Rosker, F. W. Wise, and C. L. Tang, Phys. Rev. Lett. **57**, 321 (1986).

[5] S. Ruhman, A. G. Jolly, and K. A. Nelson, J. Chem. Phys. **86**, 6563 (1987).

[6] G. L. Eesley, Phys. Rev. Lett. **51**, 2140 (1983).

[7] R. W. Schoenlein, W. Z. Lin, J. G. Fujimoto, and G. L. Eesley, Phys. Rev. Lett. **58**, 1680 (1987).

[8] Stuart D. Brorson, Ph.D. thesis, Massachusetts Institute of Technology, 1990 (unpublished).

[9] S. D. Brorson, A. Kazeroonian, J. S. Moodera, D. W. Face, T. K. Cheng, E. P. Ippen, M. S. Dresselhaus, and G. Dresselhaus, Phys. Rev. Lett. **64**, 2172 (1990).

[10] D. W. Face, S. D. Brorson, A. Kazeroonian, J. S. Moodera, T. K. Cheng, G. L. Doll, M. S. Dresselhaus, G. Dresselhaus, E. P. Ippen, T. Venkatesan, X. D. Wu, and A. Inan, IEEE Trans. Magnetics **MAG-27**, Pt. 2, 1556 (1991).

[11] T. K. Cheng, S. D. Brorson, A. S. Kazeroonian, J. S. Moodera, G. Dresselhaus, M. S. Dresselhaus, and E. P. Ippen,

Appl. Phys. Lett. **57**, 1004 (1990).
[12] G. C. Cho, W. Kütt, and H. Kurz, Phys. Rev. Lett. **65**, 764 (1990).
[13] J. M. Chwalek, C. Uher, J. F. Whitaker, G. A. Mourou, and J. A. Agostinelli, Appl. Phys. Lett. **58**, 980 (1991).
[14] T. K. Cheng, S. D. Brorson, A. Kazeroonian, J. S. Moodera, G. Dresselhaus, M. S. Dresselhaus, and E. P. Ippen, in *Extended Abstracts of the Symposium on Electronic, Optical and Device Properties of Layered Structures*, edited by J. Hayes, M. S. Hybertsen, and E. R. Weber (Materials Research Society, Pittsburgh, 1990), p. 95.
[15] H. Kurz, QELS Digest **11**, 58 (1991).
[16] T. K. Cheng, Master's thesis, Massachusetts Institute of Technology, 1990 (unpublished).
[17] T. K. Cheng, H. J. Zeiger, J. Vidal, G. Dresselhaus, M. S. Dresselhaus, and E. P. Ippen, QELS Digest **11**, 60 (1991).
[18] K. Seibert, H. Hensel, T. Albrecht, J. Gerits, K. Allenkbverdiev, and H. Kurz, *Proceedings of the 20th International Conference on the Physics of Semiconductors, Thessalonika, Greece, 1990* (International Union of Pure and Applied Physics, Göteborg, Sweden, 1990), Vol. 3, p. 1981.
[19] J. Chesnoy and A. Mokhtari, Phys. Rev. A **38**, 3566 (1988).
[20] J. A. Walmsley, F. W. Wise, and C. L. Tang, Chem. Phys. Lett. **194**, 315 (1989).
[21] J. S. Lannin, J. M. Colleja, and M. Cardona, Phys. Rev. B **12**, 585 (1975).
[22] A. S. Pine and G. Dresselhaus, Phys. Rev. B **4**, 356 (1971).
[23] S. H. Shin, R. L. Aggarwal, B. Lax, and J. M. Honig, Phys. Rev. B **9**, 583 (1974).
[24] C. S. Barrett, Australian J. Phys. **13**, 209 (1960).
[25] S. Golin, Phys. Rev. **166**, 643 (1968).
[26] D. Bohm, in *Quantum Theory* (Prentice Hall, New York, 1951), p. 306.
[27] A. J. Strauss (private communication). We are grateful to Dr. Alan Strauss of MIT Lincoln Laboratory for providing the Ti_2O_3 cyrstals.
[28] R. L. Fork, B. I. Greene, and C. V. Shank, Appl. Phys. Lett. **38**, 671 (1981).
[29] T. K. Cheng, J. Vidal, H. J. Zeiger, G. Dresselhaus, M. S. Dresselhaus, and E. P. Ippen, Appl. Phys. Lett. **59**, 1923 (1991).
[30] H. Kurz and co-workers (private communication).
[31] W. B. Pearson, in *Handbook of Lattice Spacings and Structures of Metals and Alloys*, edited by P. Villars and L. D. Calvert (American Society for Metals, Metals Park, OH, 1985).
[32] Max Born, Proc. Cambridge Philos. Soc. **36**, 160 (1940).
[33] L. L. Van Zandt, J. M. Honig, and J. B. Goodenough, J. Appl. Phys. **39**, 594 (1968).
[34] H. J. Zeiger, Phys. Rev. B **11**, 5132 (1974).

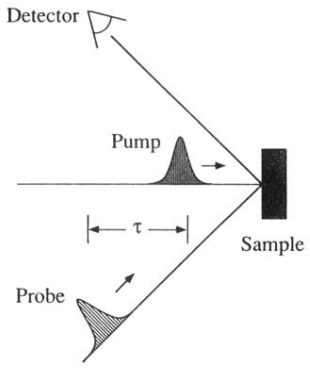

FIG. 1. Schematic diagram of the pump-probe technique used for measurement of the change in reflectivity associated with the coherent generation of optical phonons.